Simultaneous exfoliation and functionalization of MoS_2 with Tetrapyridyl Porphyrin

Electronic Supplementary Information

Marina Garrido,* ‡[a] Alejandro Criado *[b] and Maurizio Prato *[a,c,d]

[a] Department of Chemical and Pharmaceutical Sciences, Università degli Studi di Trieste, Via Licio Giorgieri 1, Trieste 34127, Italy.

[b] Universidade da Coruña, CICA – Centro Interdisciplinar de Química e Bioloxía, Rúa as Carballeiras, 15071 A Coruña, Spain.

[c] Center for Cooperative Research in Biomaterials (CIC biomaGUNE), Basque Research and Technology Alliance (BRTA), Paseo de Miramón 194, Donostia-San Sebastián 20014, Spain.

[d] Ikerbasque, Basque Foundation for Science, Bilbao 48013, Spain.

‡ Current address: IMDEA Nanociencia, Calle Faraday 9, Ciudad Universitaria de Cantoblanco, Madrid 28049, Spain.

* Corresponding author: marina.garrido@imdea.org, a.criado@udc.es, prato@units.it, mprato@cicbiomagune.es

1. Materials and methods

All reagents were purchased from commercial sources and used without further purification with the exception of pyrrole, which was filtered through an Al_2O_3 gel column prior to use to remove polymers. Nickel 5,10,15,20-tetrakis(4-pyridyl)porphyrin (NiTPyP)[1] and nickel 5,10,15,20-tetrakis(phenyl)porphyrin (NiTPP)[2] were synthesized using previously reported procedures. Thin-layer chromatography was performed on SIGMA-ALDRICH silica gel on TLC Al foils with fluorescent indicator 254 nm; chromatograms were visualized with UV light (254 and 365 nm). Column chromatography was carried out on silica gel (Merck Kieselgel 60, 230-400 mesh). Molybdenum disulfide (MoS_2, particle size < 2 µm) were purchased from SIGMA-ALDRICH. Vacuum filtrations of MoS_2 materials were carried out with polytetrafluoroethylene (PTFE) (pore size = 0.45 µm, Φ = 25 mm) membranes.

Synthesis of 5,10,15,20-tetrakis(4-pyridyl)porphyrin (TPyP):

A solution of pyrrole (2.05 mL, 29.8 mmol) and 4-pyridinecarboxaldehyde (2.80 mL, 29.8 mmol) in propionic acid (120 mL) was heated under reflux for 90 min. The mixture was cooled at room temperature, concentrated under reduced pressure, diluted with MeOH and left at -20 °C over weekend to crystalize. The obtained solid was filtered under vacuum and washed with cold MeOH to obtain the desired product as purple crystals with a yield of 17%. ^{1}H-NMR (400 MHz, $CDCl_3$) δ: 9.07 (d, 8H, J = 5.9 Hz), 8.87 (s, 8H), 8.17 (d, 8H, J = 5.9 Hz), -2.92 (s, 2H) ppm.

Synthesis of 5,10,15,20-tetrakis(phenyl)porphyrin (TPP):

A solution of pyrrole (2.05 mL, 29.8 mmol) and benzaldehyde (3.02 mL, 29.8 mmol) in propionic acid (120 mL) was heated under reflux for 30 min. The mixture was cooled at room temperature, filtered under vacuum and washed with water and MeOH to obtain the desired product as purple crystals with a yield of 23%. ^{1}H-NMR (400 MHz, $CDCl_3$) δ: 8.86 (s, 8H), 8.23 (d, 8H, J = 6.5 Hz), 7.78 (m, 12H), -2.76 (s, 2H) ppm.

Synthesis of 5,10,15,20-tetrakis(3,5-di-*tert*-butylphenyl)porphyrin (TBP):

A solution of pyrrole (0.32 mL, 4.58 mmol) and 3,5-di-*tert*-butylbenzaldehyde (1 g, 4.58 mmol) in propionic acid (18.5 mL) was heated under reflux for 90 min. The mixture was cooled at room temperature, concentrated under reduced pressure, diluted with MeOH and left at -20 °C overnight to crystalize. The obtained solid was filtered under vacuum and washed with cold MeOH to obtain the desired product as purple crystals with a yield of 9%. ^{1}H-NMR (400 MHz, $CDCl_3$) δ: 8.90 (s, 8H), 8.10 (d, 8H, J = 1.8 Hz), 7.79 (t, 4H, J = 1.8 Hz), 1.53 (s, 72H), -2.66 (s, 2H) ppm.

Synthesis of Nickel 5,10,15,20-tetrakis(3,5-di-*tert*-butylphenyl)porphyrin (NiTBP):

Nickel acetate tetrahydrate (82 mg, 0.33 mmol) was added to a solution of 5,10,15,20-tetrakis(3,5-di-*tert*-butylphenyl)porphyrin (70 mg, 0.065 mmol) in $CHCl_3$/MeOH (9/1). The mixture was bubbled with Ar during 20 minutes and then heated under reflux for 24 hours. Then the solvent was removed under reduced pressure and the crude was purified by silica gel column chromatography using petroleum ether/DCM (9/1) mixture as eluent. The product was isolated as a red solid (85%). ^{1}H-NMR (400 MHz, $CDCl_3$) δ: 8.83 (s, 8H), 7.91 (d, 8H, J = 1.8 Hz), 7.74 (t, 4H, J = 1.8 Hz), 1.50 (s, 72H) ppm.

Exfoliation procedure with TPyP:

To a solution of TPyP (5 mg) in $CHCl_3$ (20 mL) were added 20 mg of MoS_2, then the mixture was sonicated during 150 min in a sonication bath with an ice/water bath to avoid the increase of temperature. The suspension was centrifuged at 20°C during 45 min at 500 r.p.m., then the supernatant was collected and characterized. For the characterization, 0.1 mL of the initial supernatant dispersion were diluted in 3 mL of $CHCl_3$, this dispersion was employed for all the analyses except for the TGA, IR and XPS measures. **Amount of MoS_2 in the supernatant**: was calculated in terms of weight respect to bulk MoS_2 with the weight loss observed in the TGA profile at 600°C (56.3%). The supernatant was filtered obtaining 7.03 mg of material, resulting in 3.96 mg of TPyP, and therefore in an exfoliation degree of 15%. The **functionalization degree** (FD) was calculated at 600 °C employing the TGA profile. FD is defined as number of MoS_2 molecules per introduced functional group, $FD = \frac{R\,(\%)\cdot M_W(g/mol)}{L\,(\%)\cdot 160.07(g(mol)}$. Where R and L correspond to the residue (%) and the weight loss (%) observed at 600 °C. The expected moiety on the MoS_2 surface is expressed as (M_W) and the molecular weight of MoS_2 determined to be 160.07 g/mol.

The same procedure was used to obtain the dispersion of MoS_2 in $CHCl_3$ employed in the different experiments in which the bare MoS_2 is required. To verify the stability of $CHCl_3$ during the sonication process, no acidification, the dispersion of MoS_2 was filtered and then employed to corroborate that the changes observed in the UV-Vis titration experiments are due to the interactions between the porphyrins and MoS_2, and non to the protonation of the porphyrins as

a consequence of the acidify $CHCl_3$ (Figure S23). As expected, the UV-Vis spectra obtained in this titration are the dilution ones.

To determine the stability of TPyP during the sonication process, a solution of TPyP (5 mg) in $CHCl_3$ (20 mL) was sonicated during 150 min in a sonication bath with an ice/water bath to avoid the increase of temperature. In Figure S24 is shown the UV-Vis spectrum of TPyP after the sonication process, the characteristic Soret band of the free porphyrin is still present confirming its stability.

To study the effect of the solvent in the interactions between TPyP and MoS_2, the same exfoliation procedure detailed in the case of $CHCl_3$ was employed with the other investigated solvents (Figure S7).

2. Instruments

^{1}H-NMR spectra were recorded at 400 MHz (Varian 400 spectrometer). Raman spectra were recorded on a Renishaw inVia Raman Microscope at room temperature using an exciting laser source of 785 nm. TEM micrographs were obtained using a Philips EM208 TEM and RADIUS 2.0 software (EMSIS GmbH, Muenster, Germany). The samples were dispersed in $CHCl_3$ and dropped onto a lacey carbon copper grid (300 mesh), the solvent was removed at room temperature overnight. AFM was performed under ambient conditions using Multimode V7.30 (Veeco Instruments Inc., Santa Barbara, USA) with a NanoScope V controller (Digital Instruments, Santa Barbara, USA) working on tapping mode with a silicon tip (HQ:NSC15/Al BS probes from Mikromasch) at a working frequency of 235 KHz and a nominal force constant of 40 Nm^{-1}. Height and phase images were simultaneously obtained. The samples were prepared by spin coating on silicon surfaces and were dried under ambient conditions overnight. UV-Vis-NIR measurements were carried out on a Cary 5000 Spectrometer (Varian), using 1 cm path quartz cuvettes. FTIR spectra were carried out in a Perkin Elmer System 2000 NIR FT-Raman using a spectral range of 4000–370 cm^{-1}, with a resolution of 4 cm^{-1}, and in pellets of dispersed samples of the corresponding materials in dried KBr. Fluorescence measurements were carried out on a Cary Eclipse Fluorescence Spectrophotometer (Varian), using 1 cm path quartz cuvettes. TGA measurements were performed with a TGA Q500 (TA Instruments) under a N_2 atmosphere. The samples were introduced inside a platinum crucible and equilibrated at 100 °C followed by a 10 °C/min ramp between 100 and 800 °C. XPS measurements were performed in a SPECS Sage HR 100 spectrometer with a nonmonochromatic X-ray source of aluminium with a Kα line of 1486.6 eV energy and 300 W. The fitting of the XPS data was applied using CasaXPS software. EDS experiments were carried out using a Sigma 300 VP microscope (Zeiss), using a SE2 detector, at 6 kV, 8.5 mm working distance and 120 µm aperture size. The analyzed samples are the one prepared for AFM.

3. Supporting Images and Tables

Table S1: Conditions for MoS_2 LPE procedures reported.

Method	Solvent	Molecule	Time	Ref.
Ball-milling and sonication	Water	SDS	12 h ball-milling and 2 h sonication	[3]
Sonic tip	Water	SC	30 min	[4]
Sonic tip	THF and Cyclohexanone	Different polymers	30 min	[5]
Sonication bath	Water	TRPIL (ionic liquid)	18 h	[6]
Sonic tip	Water	Different polyphenols	2 h	[7]
Sonic bath	Water DMF DMSO MeOH	PIL (poly (ionic liquid))	1 h	[8]
Sonic bath	Water	**Pyrene derivatives**	**48 h**	[9]
Sonic bath	Water THF	**Hexahydroxytriphenylene derivatives**	**72 h**	[10]

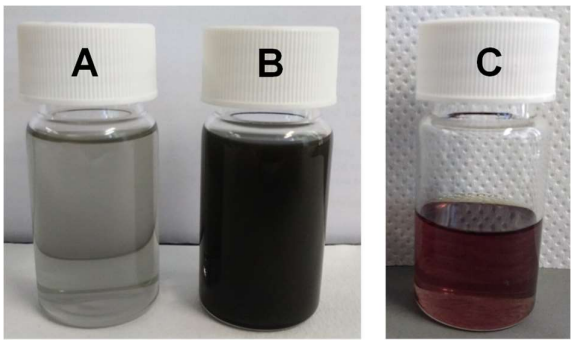

Figure S1: Dispersions of MoS_2 obtained through LPE in $CHCl_3$ A) in the absence of TPyP, B) in the presence of TPyP and C) a solution of TPyP in $CHCl_3$.

Table S2. Different conditions tested for the developed methodology.

MoS_2 (mg)	TPyP (mg)	$CHCl_3$ (mL)	Sonication (min)	Exciton A and B (nm)
20	5	10	60	688 / 641
20	5	10	150	681 / 620
20	5	20	150	678 / 617
10	2.5	5	150	683 / 622
32	8	5	150	688 / 639

The optimal conditions for the developed procedure were determined by the value of the A exciton of MoS_2, since it is related to the thickness of the obtained flakes.[11] As it can be observed in Table S2, the smaller value was obtained by mixing 20 mg of MoS_2 and 5 mg of TPyP in 20 mL of $CHCl_3$ and sonicating during 150 min.

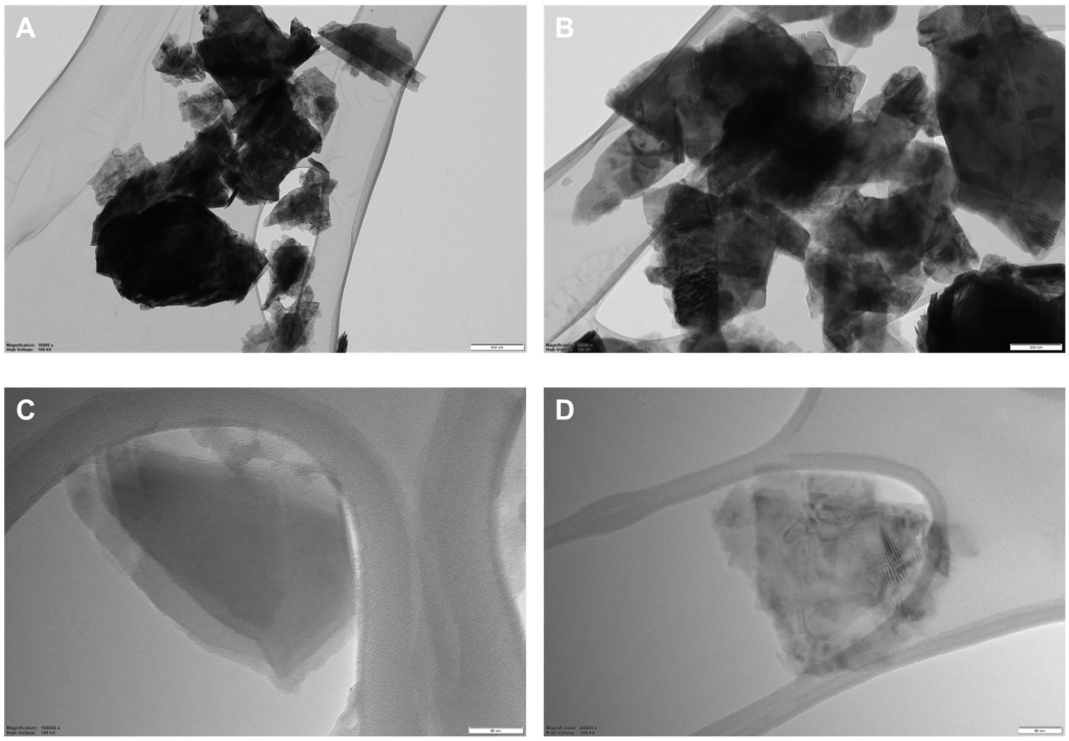

Figure S2: Representative TEM images of A), B) bulk MoS_2, the scale bar is 500 and 200 nm, respectively, and C), D) of the obtained material after LPE, the scale bar is 50 nm.

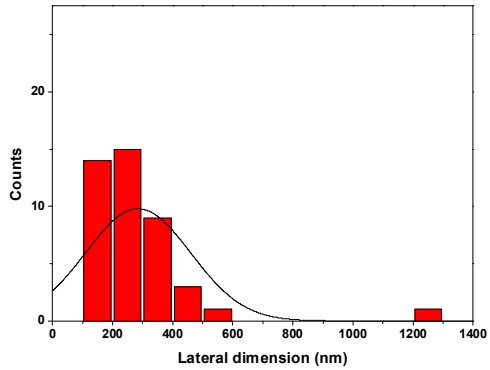

Figure S3: Lateral dimension distribution from TEM images of the obtained material after LPE.

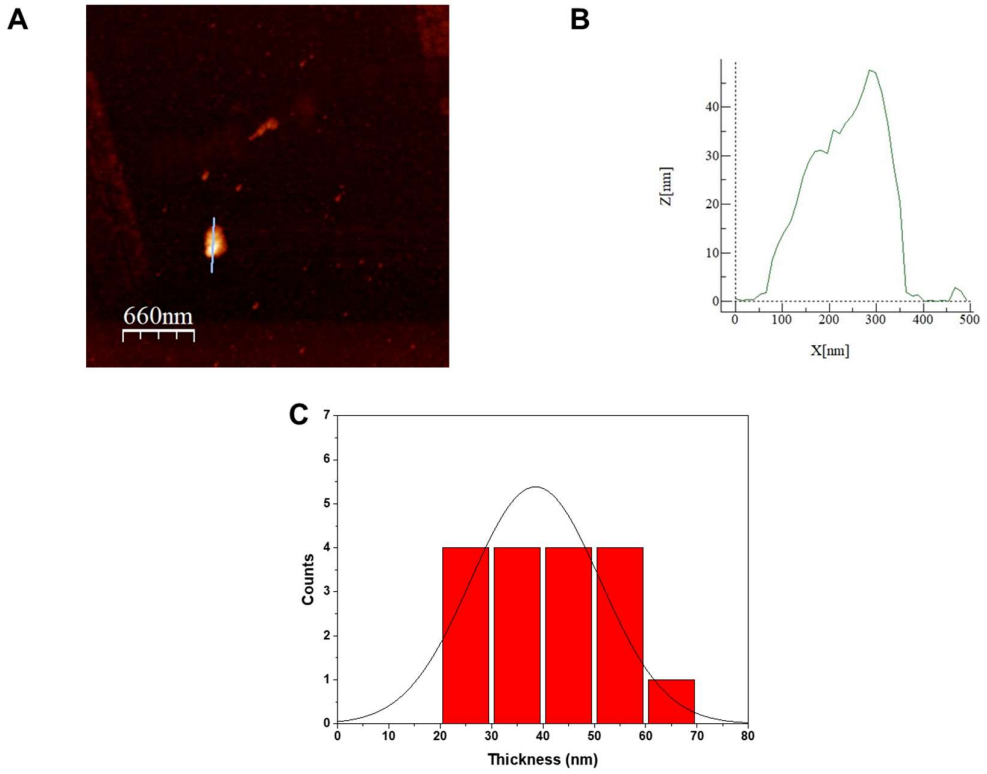

Figure S4. A) AFM image and B) the corresponding high profile of bulk MoS_2. C) Thickness distribution of bulk MoS_2.

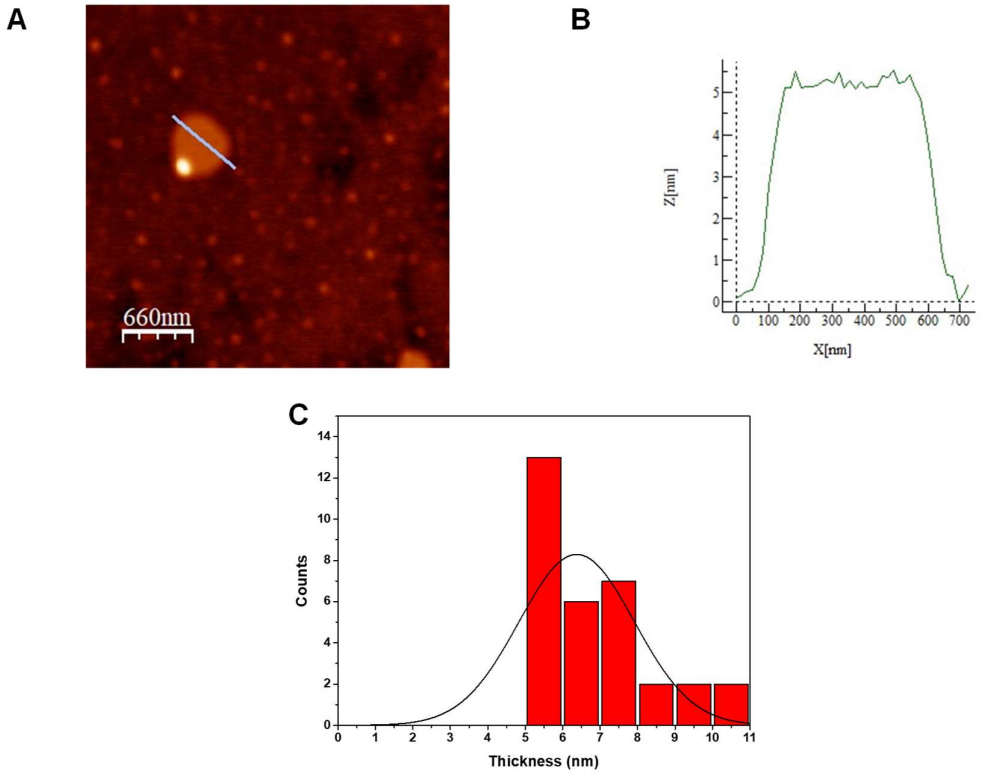

Figure S5: A) AFM image and B) the corresponding high profile of the obtained material after LPE. C) Thickness distribution of the obtained material after LPE.

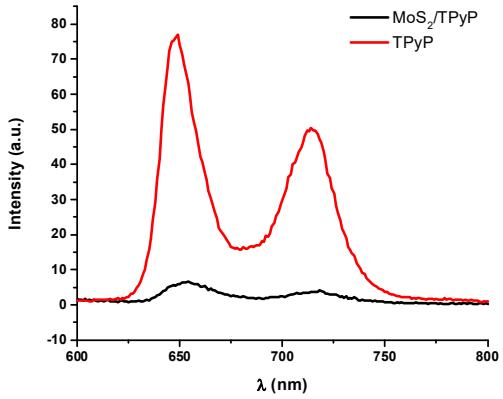

Figure S6: Fluorescence spectra (λ_{exc} = 417 nm) of MoS_2/TPyP (black) and TPyP (red, $3 \cdot 10^{-6}$ M) in $CHCl_3$.

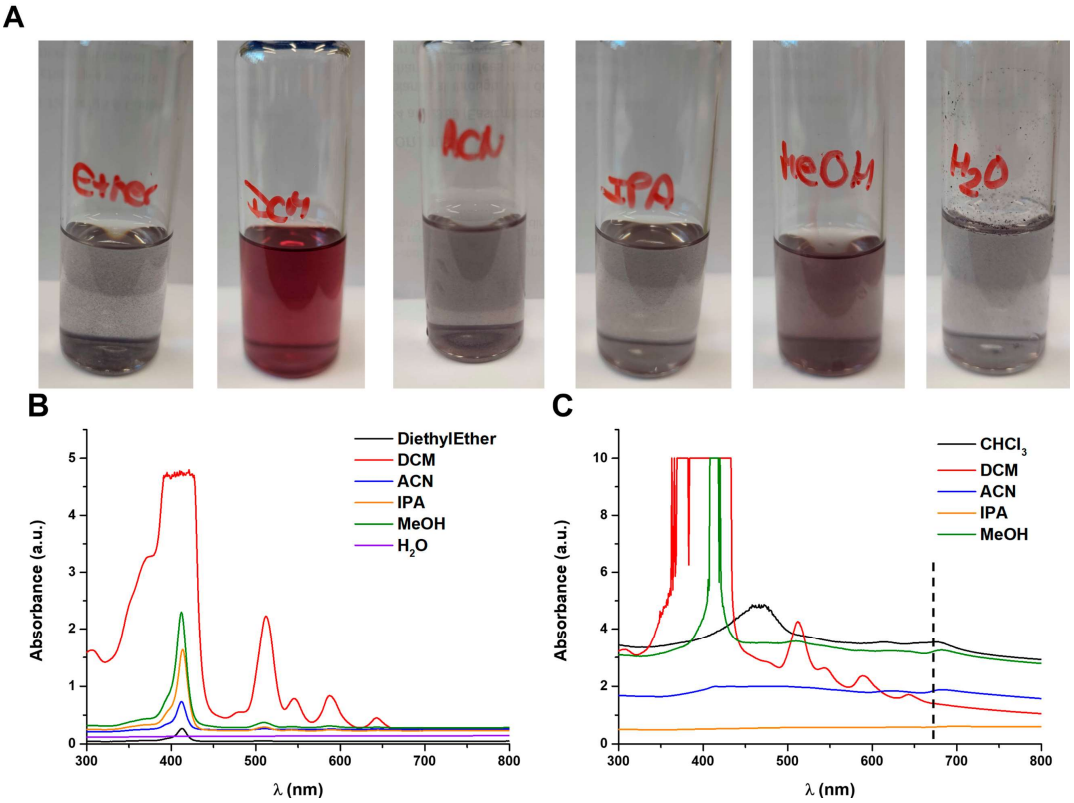

Figure S7: A) Solubility of TPyP (0.25 mg/mL) in different low boiling point solvents. B) UV-Vis spectra of TPyP in different low boiling point solvents. C) UV-Vis spectra of MoS_2/TPyP supernatant in different low boiling points solvents recorded without dilution.

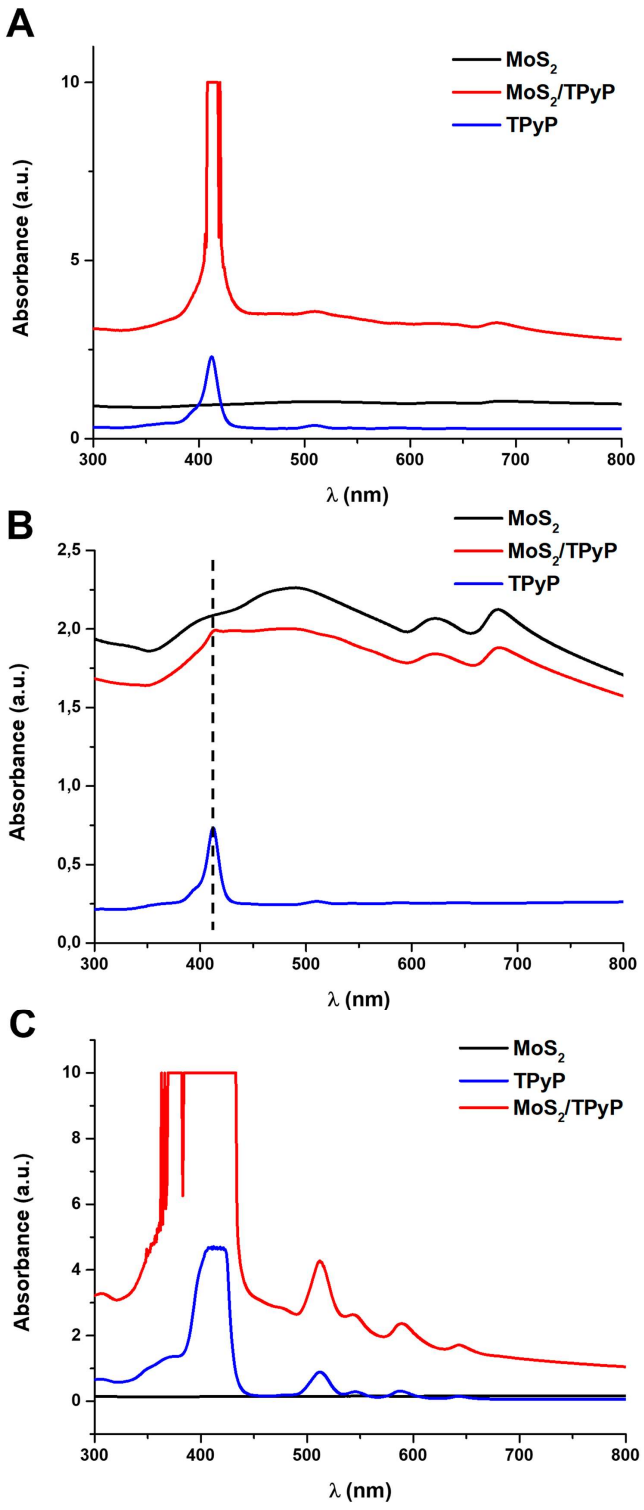

Figure S8: UV-Vis spectra of MoS_2 (black), MoS_2/TPyP (red) and TPyP (blue) in A) MeOH, B) ACN and C) DCM.

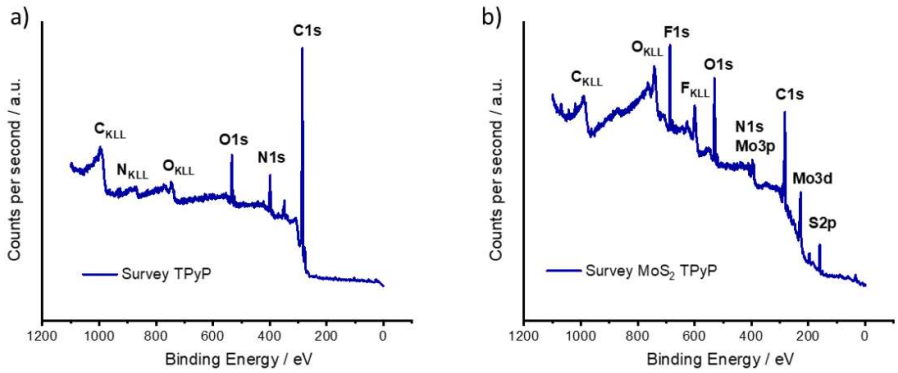

Figure S9: Survey spectra for (a) TPyP and (b) MoS_2/TPyP. For MoS_2/TPyP, the detected F signals are from the PTFE membrane on which the sample was analyzed.

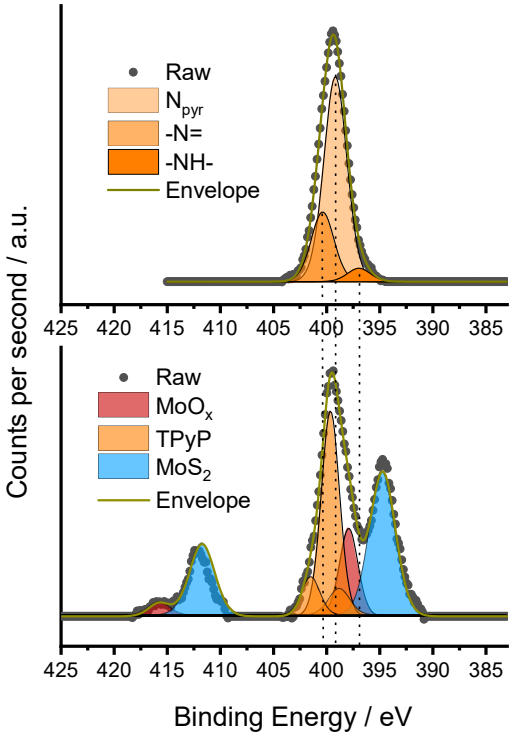

Figure S10: Deconvoluted N1s and Mo3p core levels for TPyP (top) and MoS_2/TPyP (down).

Table S3: N1s and Mo3p core level components for TPyP and MoS_2/TPyP.

Sample	Component	Position / eV	FWHM	At%
TPyP	-NH-	400.0	2.53	24.2
	Npyr	398.8	2.53	71.2
	-N=	396.6	2.53	4.6
MoS_2/TPyP	-NH-	401.4	2.03	9.3
	Npyr	399.6	2.03	49.7
	-N=	397.9	2.03	21.3
	MoS_2 (Mo3p3/2)	394.7	2.81	11.4
	MoS_2 (Mo3p1/2)	411.7	2.81	5.7
	MoO_x (Mo3p3/2)	398.7	2.37	1.8
	MoO_x (Mo3p1/2)	415.7	2.37	0.9

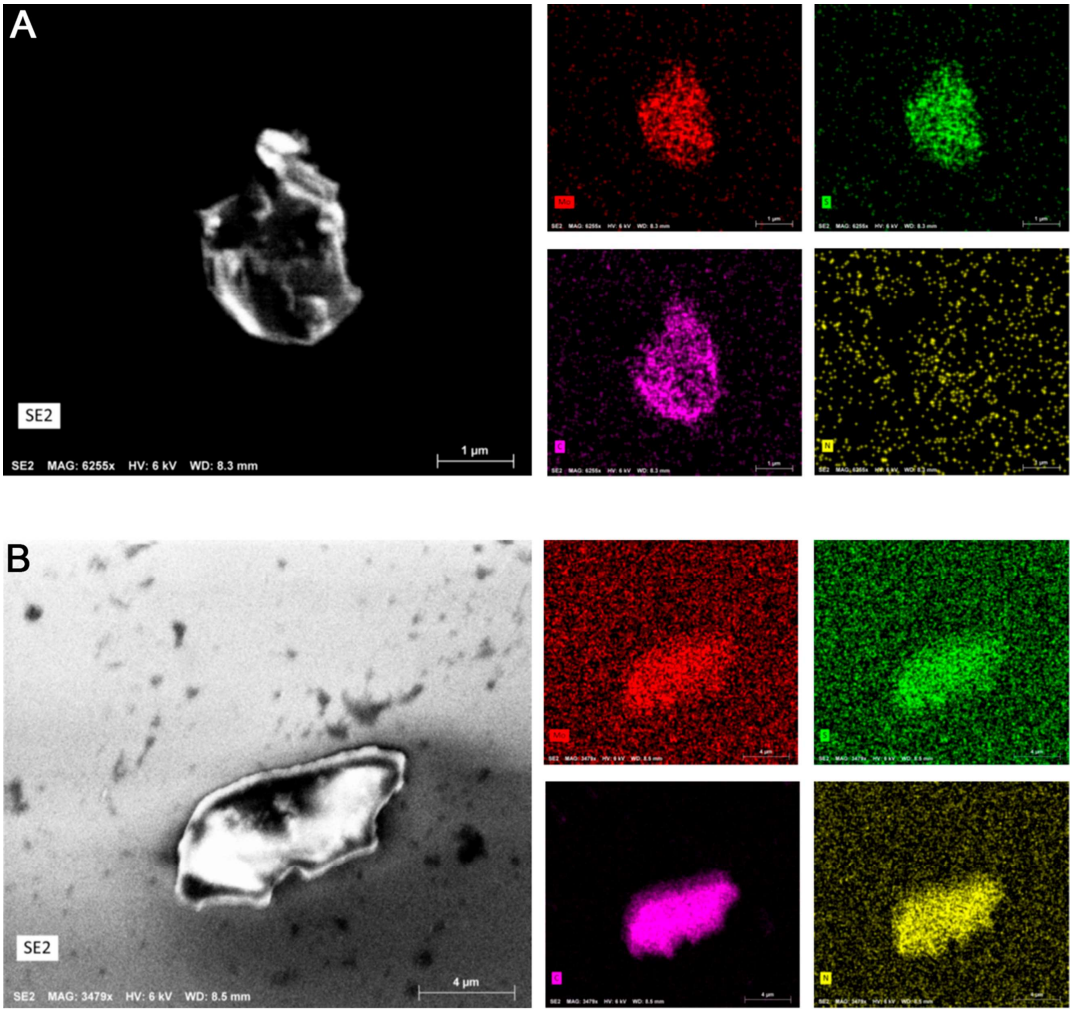

Figure S11: Representative SEM images of A) bulk MoS_2 and B) MoS_2/TPyP. EDS maps for the elemental distribution of Mo (red), S (green), C (pink) and N (yellow).

The presence of C in bulk MoS_2 could be due to the presence of residual $CHCl_3$, since is the solvent employ to prepare the samples.

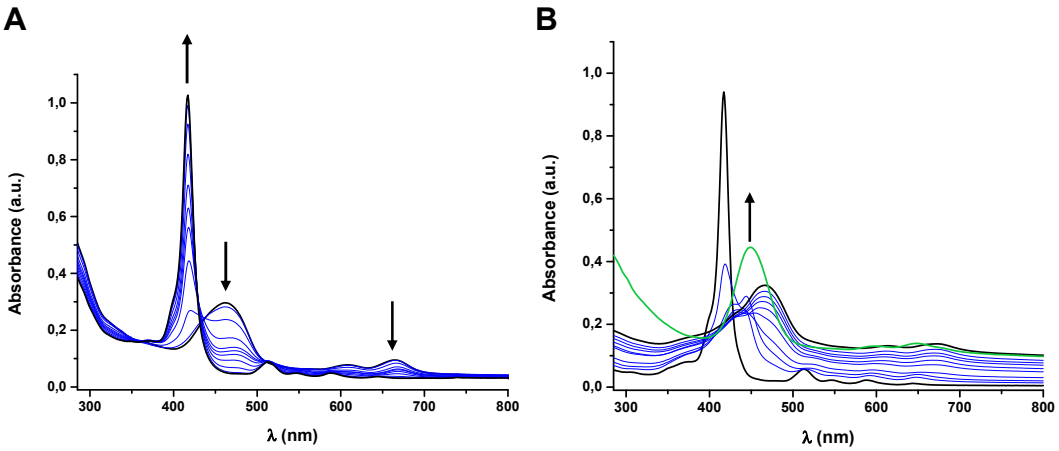

Figure S12: UV-Vis spectra of A) TPyP ($3 \cdot 10^{-6}$ M) obtained when increasing amounts of MeOH were added to the final point of the titration with MoS_2, and B) TPyP ($3 \cdot 10^{-6}$ M) obtained during the titration with MoS_2 with the final addition of 50 µL of TFA (spectrum in green). Both titrations were performed in $CHCl_3$. Each addition corresponds to 100 µL.

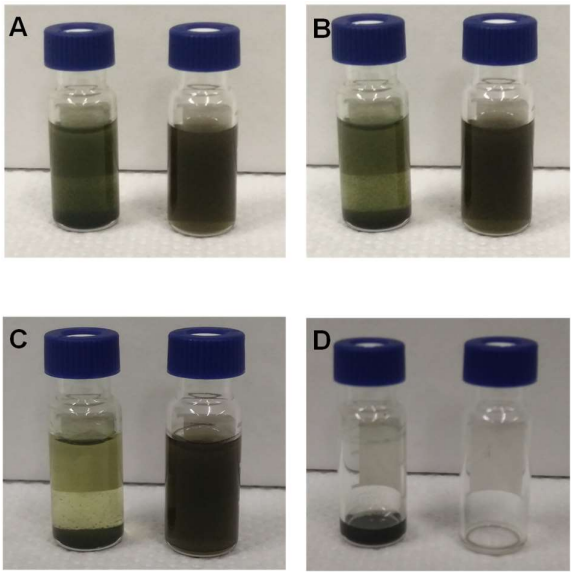

Figure S13: Stability of the dispersion of MoS_2/TPyP in the presence (left vial) and in the absence of TFA (right vial) during 2 hours. The breaking of the interaction between TPyP and MoS_2 results in the precipitation of the material after the addition of 50 µL of TFA.

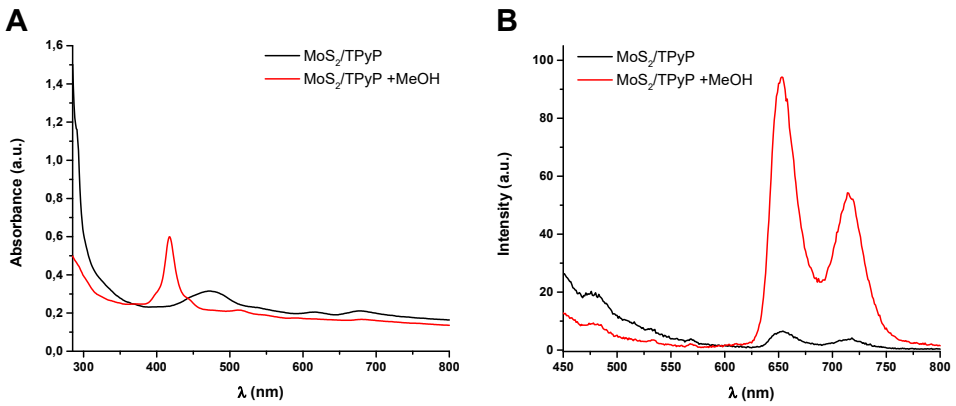

Figure S14: A) UV-Vis and B) fluorescence spectra of MoS_2/TPyP in $CHCl_3$ after the addition of 0.5 mL of MeOH.

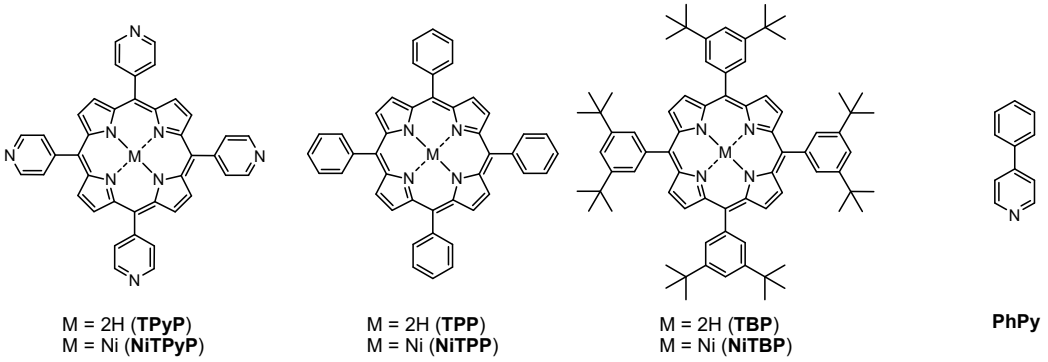

Figure S15: Molecular structures of the porphyrins and 4-phenylpyridine employed for the additional UV-Vis titrations.

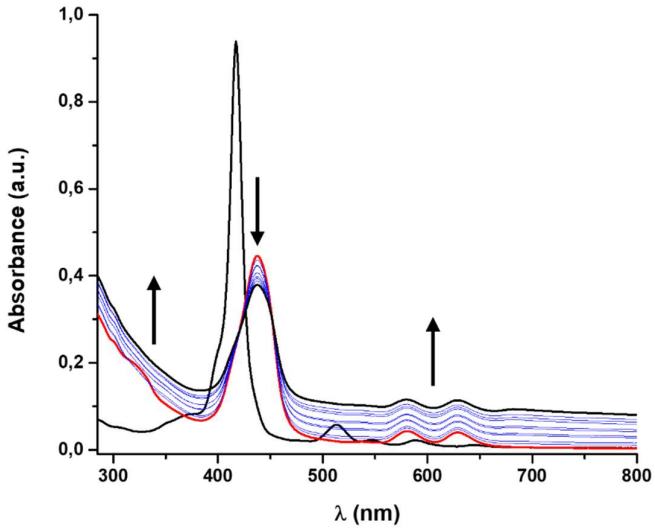

Figure S16: UV-Vis spectra of protonated TPyP ($3 \cdot 10^{-6}$ M, red line) obtained when increasing amounts of MoS_2 were added. The titration was performed in $CHCl_3$. Each addition corresponds to 20 µL. TPyP was protonated with 50 µL of TFA.

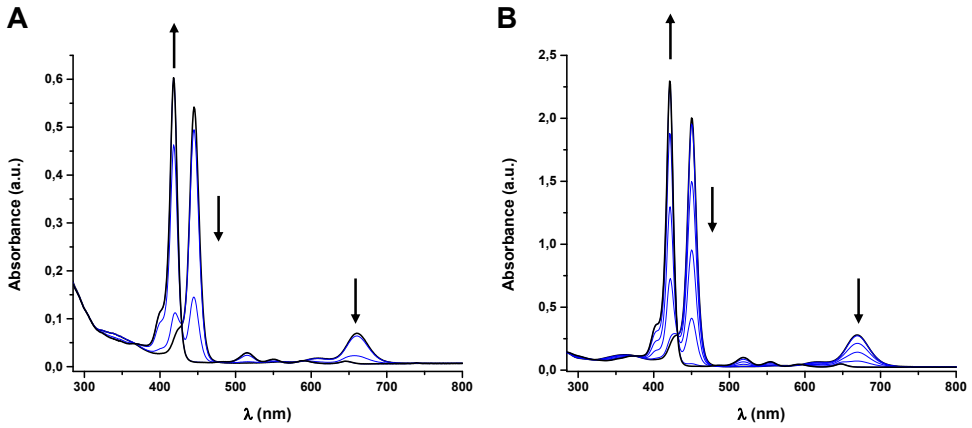

Figure S17: UV-Vis spectra of A) TPP and B) TBP ($3 \cdot 10^{-6}$ M) obtained when increasing amounts of MeOH were added to the final point of the titration with MoS_2. Both titrations were performed in $CHCl_3$. Each addition corresponds to 50 µL.

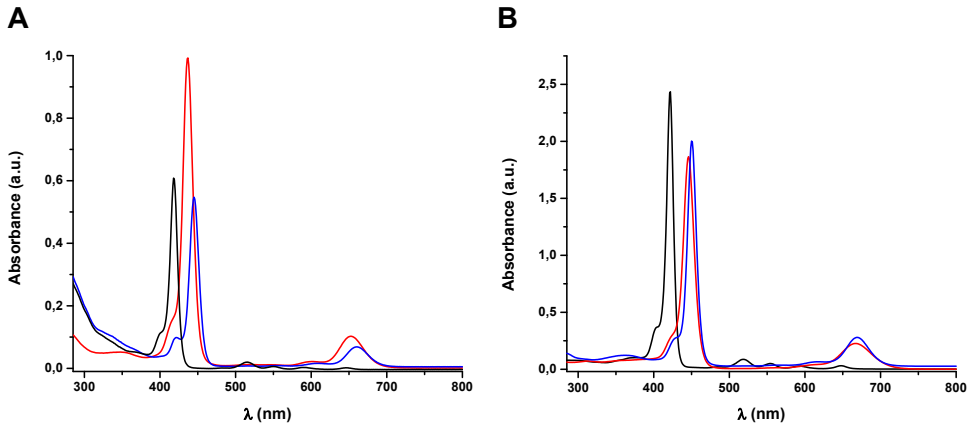

Figure S18: UV-Vis spectra of A) TPP and B) TBP ($3 \cdot 10^{-6}$ M) in $CHCl_3$. The black spectra correspond to the free porphyrins, the red spectra are registered after the addition of 50 µL of TFA and the blue spectra after the addition of 200 µL of a dispersion of MoS_2.

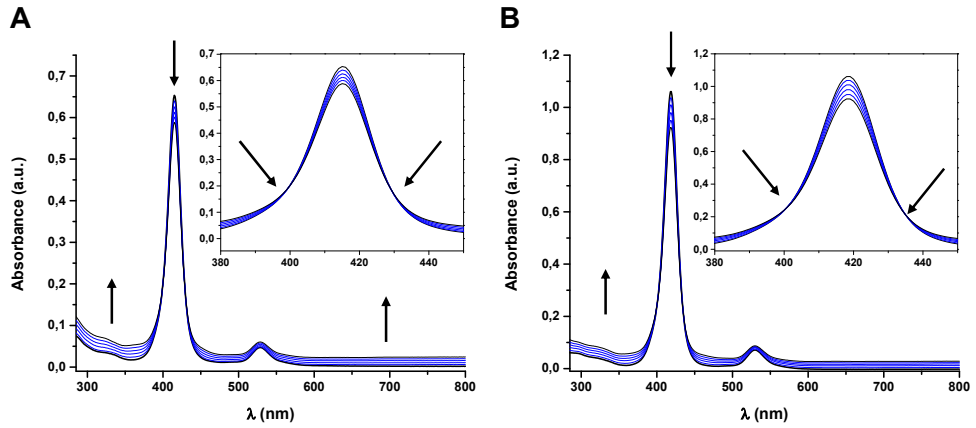

Figure S19: UV-Vis spectra obtained during the titration with MoS_2 of A) NiTPP and B) NiTBP ($3 \cdot 10^{-6}$ M) in $CHCl_3$. Each addition corresponds to 100 µL.

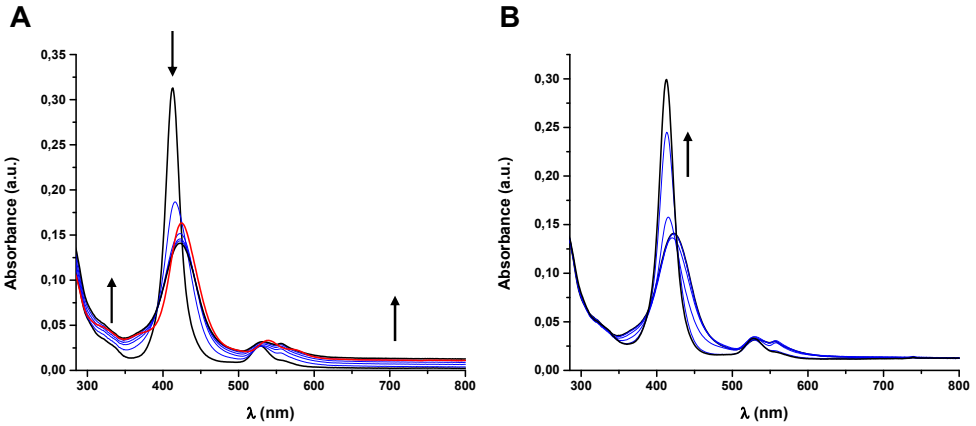

Figure S20: UV-Vis spectra of A) NiTPyP ($3 \cdot 10^{-6}$ M) during the titration with MoS_2 with the final addition of 50 µL of TFA (spectrum in red). B) NiTPyP ($3 \cdot 10^{-6}$ M) obtained when increasing amounts of MeOH were added to the final point of the titration with MoS_2. Both titrations were performed in $CHCl_3$. Each addition corresponds to 20 µL.

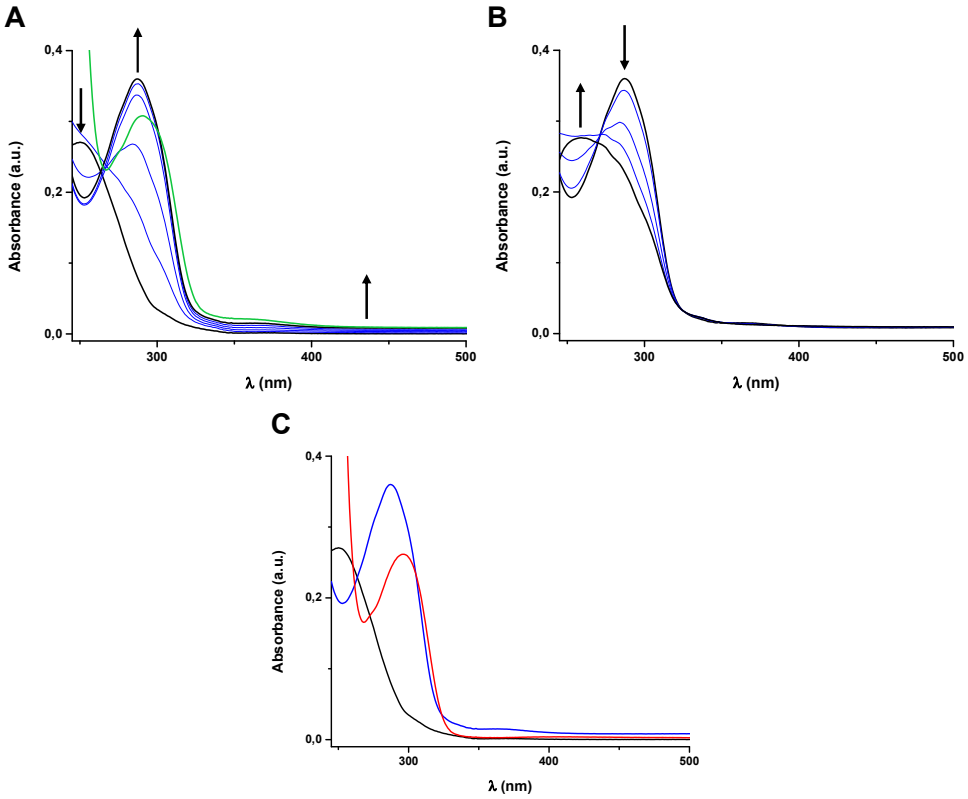

Figure S21: UV-Vis spectra of A) 4-phenylpyridine ($3 \cdot 10^{-6}$ M) during the titration with MoS_2 with the final addition of 100 µL of TFA (spectrum in green). B) 4-Phenylpyridine ($3 \cdot 10^{-6}$ M) obtained when increasing amounts of MeOH were added to the final point of the titration with MoS_2. Both titrations were performed in $CHCl_3$. In the case of the titration with MoS_2, each addition corresponds to 20 µL. For the experiments with MeOH, each addition corresponds to 40 µL, except the last addition that corresponds with a final added volume of 240 µL. C) UV-Vis spectra of 4-phenylpyridine ($3 \cdot 10^{-6}$ M) in $CHCl_3$. The black spectrum corresponds to the molecule, the red spectrum is registered after the addition of 200 µL of TFA and the blue spectrum after the addition of 100 µL of a dispersion of MoS_2.

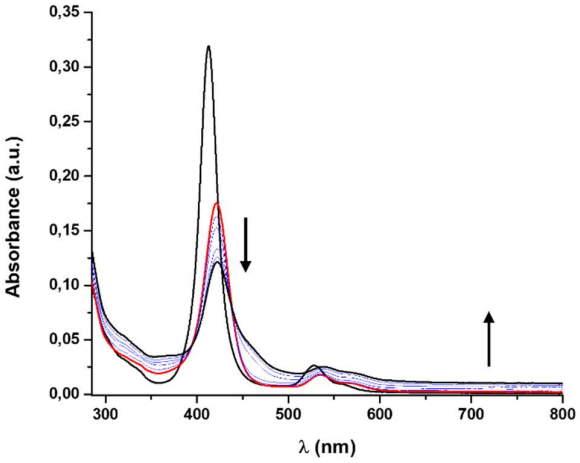

Figure S22: UV-Vis spectra of protonated NiTPyP ($3 \cdot 10^{-6}$ M, red line) obtained when increasing amounts of MoS_2 were added. The titration was performed in $CHCl_3$. Each addition corresponds to 20 µL. NiTPyP was protonated with 100 µL of TFA.

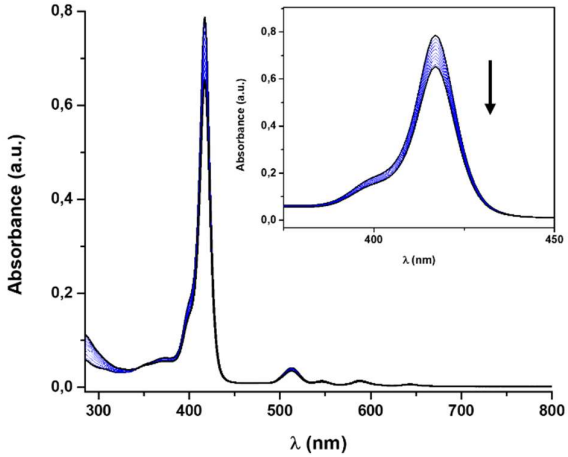

Figure S23: UV-Vis spectra of TPyP ($3 \cdot 10^{-6}$ M) obtained when increasing amounts of a filtered dispersion of MoS_2 were added. The titration was performed in $CHCl_3$. Each addition corresponds to 100 µL.

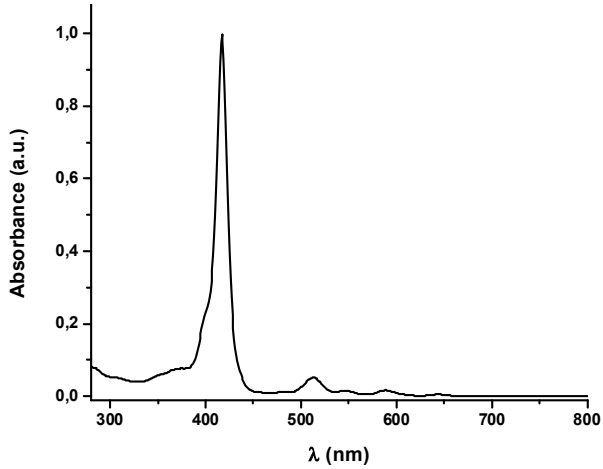

Figure S24: UV-Vis spectrum of TPyP in $CHCl_3$ ($3 \cdot 10^{-6}$ M) obtained after the dilution of the solution sonicated during 150 min.

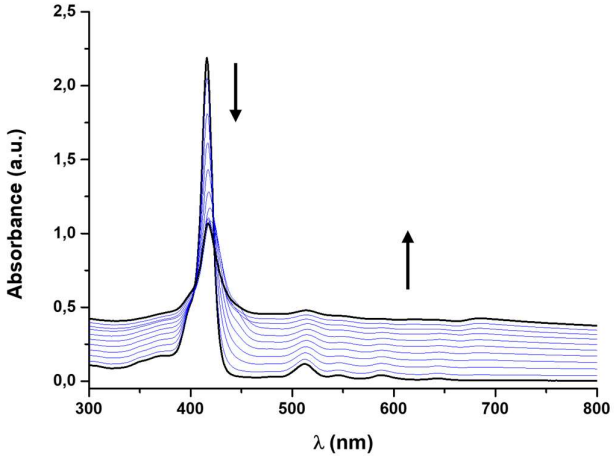

Figure S25. UV-Vis spectra obtained during the titration with MoS_2 of TPyP ($3 \cdot 10^{-6}$ M) in DCM. Each addition corresponds to 100 µL.

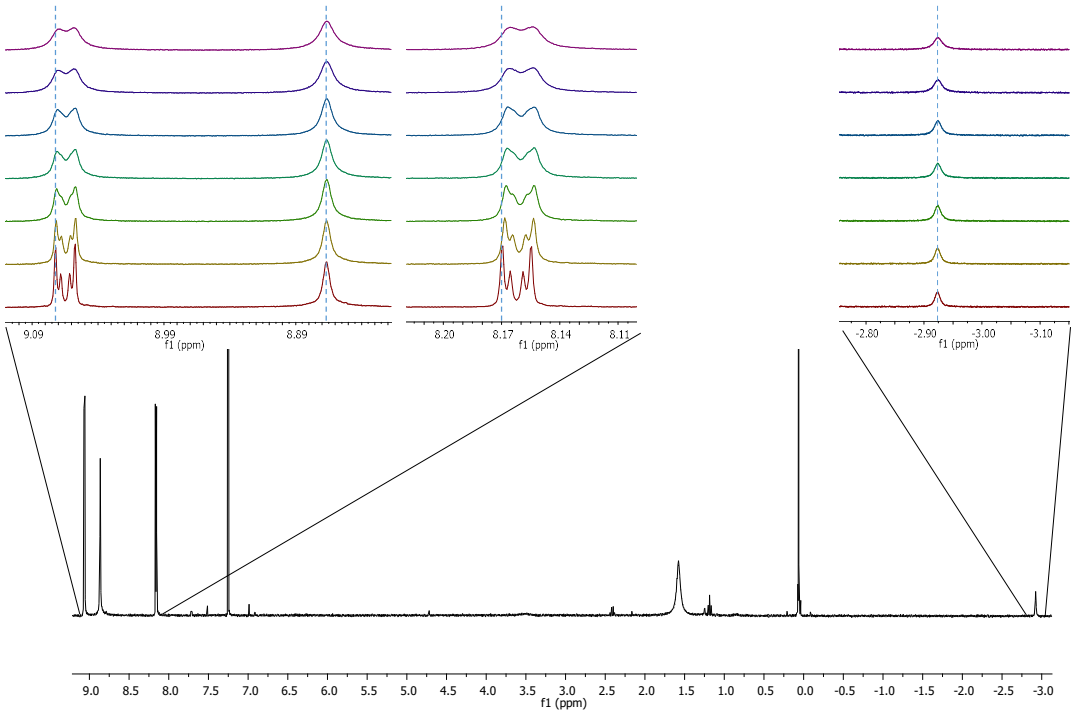

Figure S26: ^{1}H-NMR (400 MHz, $CDCl_3$, 298 K) spectra of TPyP ($2.5 \cdot 10^{-3}$ M) obtained during the titration with MoS_2. Each addition corresponds to 1 mg of MoS_2.

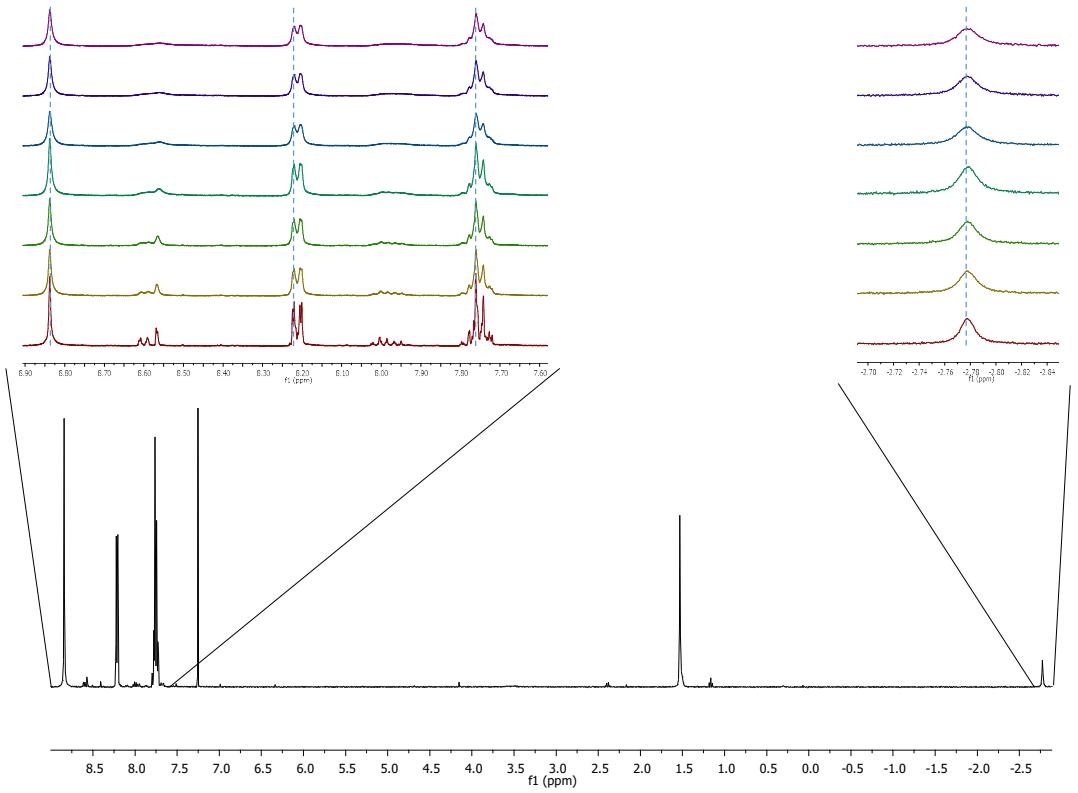

Figure S27: ^{1}H-NMR (400 MHz, $CDCl_3$, 298 K) spectra of TPP ($2.5 \cdot 10^{-3}$ M) obtained during the titration with MoS_2. Each addition corresponds to 1 mg of MoS_2.

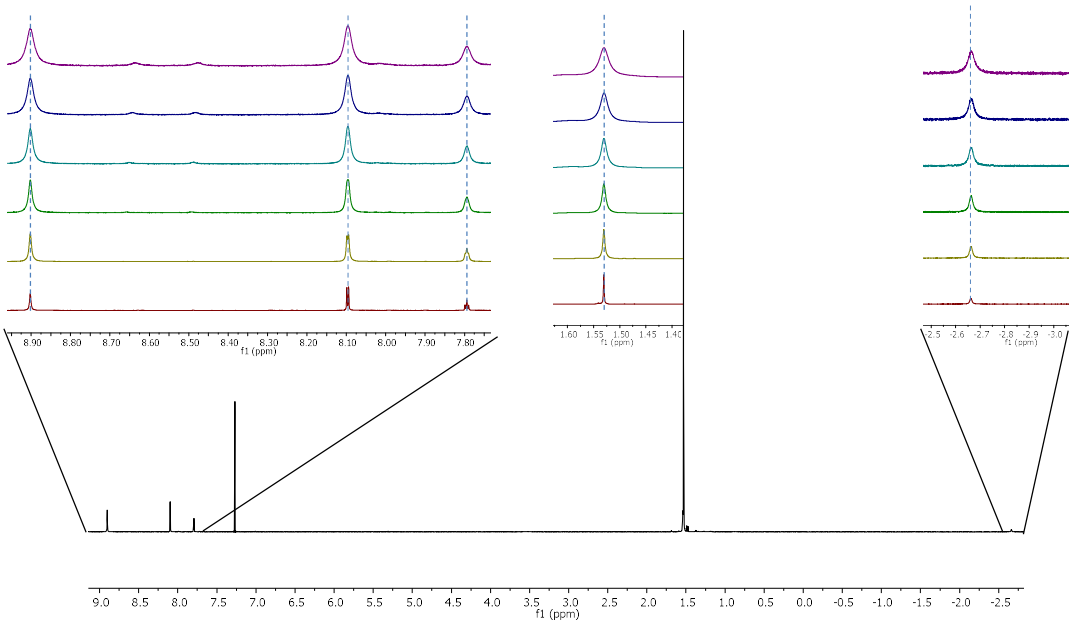

Figure S28: ^{1}H-NMR (400 MHz, $CDCl_3$, 298 K) spectra of TBP ($2.5 \cdot 10^{-3}$ M) obtained during the titration with MoS_2. Each addition corresponds to 1 mg of MoS_2.

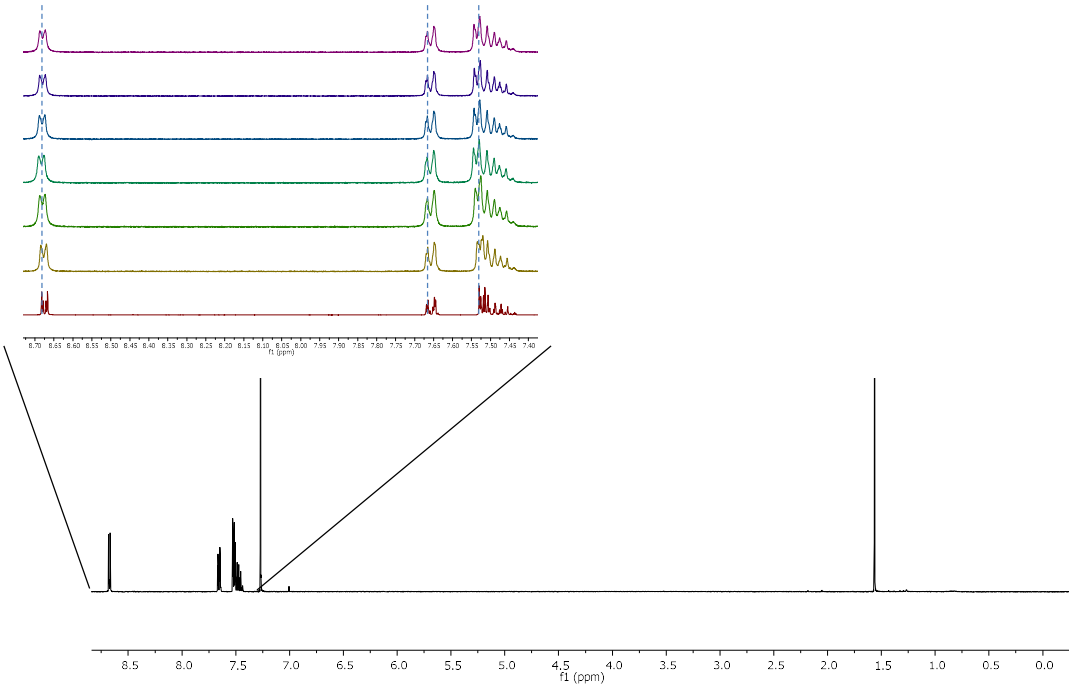

Figure S29: ^{1}H-NMR (400 MHz, $CDCl_3$, 298 K) spectra of 4-phenylpyridine ($2.5 \cdot 10^{-3}$ M) obtained during the titration with MoS_2. Each addition corresponds to 1 mg of MoS_2.

4. References

(1) Muratsugu, S.; Yamaguchi, A.; Yokota, G.; Maeno, T.; Tada, M. Tuning the Structure and Catalytic Activity of Ru Nanoparticle Catalysts by Single 3d Transition-Metal Atoms in Ru12–Metalloporphyrin Precursors. *Chem. Commun.* **2018**, *54* (38), 4842–4845. https://doi.org/10.1039/C7CC09862F.

(2) Mandal, T.; Das, S.; De Sarkar, S. Nickel(II) Tetraphenylporphyrin as an Efficient Photocatalyst Featuring Visible Light Promoted Dual Redox Activities. *Adv. Synth. Catal.* **2019**, *361* (13), 3200–3209. https://doi.org/https://doi.org/10.1002/adsc.201801737.

(3) Yao, Y.; Lin, Z.; Li, Z.; Song, X.; Moon, K.-S.; Wong, C. Large-Scale Production of Two-Dimensional Nanosheets. *J. Mater. Chem.* **2012**, *22* (27), 13494–13499. https://doi.org/10.1039/C2JM30587A.

(4) Smith, R. J.; King, P. J.; Lotya, M.; Wirtz, C.; Khan, U.; De, S.; O'Neill, A.; Duesberg, G. S.; Grunlan, J. C.; Moriarty, G.; Chen, J.; Wang, J.; Minett, A. I.; Nicolosi, V.; Coleman, J. N. Large-Scale Exfoliation of Inorganic Layered Compounds in Aqueous Surfactant Solutions. *Adv. Mater.* **2011**, *23* (34), 3944–3948. https://doi.org/10.1002/adma.201102584.

(5) May, P.; Khan, U.; Hughes, J. M.; Coleman, J. N. Role of Solubility Parameters in Understanding the Steric Stabilization of Exfoliated Two-Dimensional Nanosheets by Adsorbed Polymers. *J. Phys. Chem. C* **2012**, *116* (20), 11393–11400. https://doi.org/10.1021/jp302365w.

(6) Wang, X.; Wu, P. Aqueous Phase Exfoliation of Two-Dimensional Materials Assisted by Thermoresponsive Polymeric Ionic Liquid and Their Applications in Stimuli-Responsive Hydrogels and Highly Thermally Conductive Films. *ACS Appl. Mater. Interfaces* **2018**, *10* (3), 2504–2514. https://doi.org/10.1021/acsami.7b15712.

(7) Zhang, C.; Hu, D.-F.; Xu, J.-W.; Ma, M.-Q.; Xing, H.; Yao, K.; Ji, J.; Xu, Z.-K. Polyphenol-Assisted Exfoliation of Transition Metal Dichalcogenides into Nanosheets as Photothermal Nanocarriers for Enhanced Antibiofilm Activity. *ACS Nano* **2018**, *12* (12), 12347–12356. https://doi.org/10.1021/acsnano.8b06321.

(8) Biswas, Y.; Dule, M.; Mandal, T. K. Poly(Ionic Liquid)-Promoted Solvent-Borne Efficient Exfoliation of MoS2/MoSe2 Nanosheets for Dual-Responsive Dispersion and Polymer Nanocomposites. *J. Phys. Chem. C* **2017**, *121* (8), 4747–4759. https://doi.org/10.1021/acs.jpcc.7b00952.

(9) Yang, H.; Withers, F.; Gebremedhn, E.; Lewis, E.; Britnell, L.; Felten, A.; Palermo, V.; Haigh, S.; Beljonne, D.; Casiraghi, C. Dielectric Nanosheets Made by Liquid-Phase Exfoliation in Water and Their Use in Graphene-Based Electronics. *2D Mater.* **2014**, *1* (1), 011012. https://doi.org/10.1088/2053-1583/1/1/011012.

(10) Gang, L.; Naoki, K. Efficient and Scalable Production of 2D Material Dispersions Using Hexahydroxytriphenylene as a Versatile Exfoliant and Dispersant. *ChemPhysChem* **2016**, *17* (11), 1557–1567. https://doi.org/10.1002/cphc.201600187.

(11) Backes, C.; Smith, R. J.; McEvoy, N.; Berner, N. C.; McCloskey, D.; Nerl, H. C.; O'Neill, A.; King, P. J.; Higgins, T.; Hanlon, D.; Scheuschner, N.; Maultzsch, J.; Houben, L.; Duesberg, G. S.; Donegan, J. F.; Nicolosi, V.; Coleman, J. N. Edge and Confinement Effects Allow in Situ Measurement of Size and Thickness of Liquid-Exfoliated Nanosheets. *Nat. Commun.* **2014**, *5* (1), 4576. https://doi.org/10.1038/ncomms5576.